Presented at the 16th Symposium on the Coastal Environment, 98th AMS Annual Meeting, Austin, TX, Jan 7-11, 2018

6.3 EVALUATION AND CHALLENGES USING THE NEARSHORE WAVE PREDICTION SYSTEM IN HAWAII THROUGH THE 2016-2017 WINTER SEASON

Alex Gibbs, Andre van der Westhuysen, Stylianos Flampouris, Patrick Caldwell, Pablo Santos, Roberto Padilla-Hernandez

1. INTRODUCTION

An evaluation of the Nearshore Wave Prediction System (NWPS, Van der Westhuysen et al. 2016) in the Hawaiian Islands during a winter season is a critical step in determining the validity of the system in a swell-dominated region. It also aims to distinguish any trends or biases to take into account during operational marine forecasting. The wave model SWAN (Booij et al. 1999), is used as the nearshore wave model within NWPS, and includes the global operational multi-gridded WAVEWATCH III® wave model (WW3, Tolman et al. 2002; Chawla et al. 2013) for boundary conditions. The model is run on-demand and uses wind input from the National Weather Service (NWS) Forecast Office in Honolulu, HI to ensure wind and wave consistency in the operational marine forecasts.

This paper presents a seasonal validation of the NWPS for the 2016-2017 winter period along the North Shore of Oahu. Nearshore observations from the Pacific Islands Ocean Observing System (PacIOOS) Datawell Waverider buoy, positioned near Waimea Bay along the North Shore of Oahu, are used to evaluate the modeling system. The validation results show that the model performs sufficiently well overall, with a mean absolute error (MAE) for significant wave height of 0.25 m and a mean error of -0.02 m. However, the analysis also reveals systematic problem areas related to model biases with large swell events. Considering the nested nature of the high-resolution NWPS domain over Hawaii, these biases are in turn strongly related to the accuracy of the offshore wave boundary conditions received from the global WW3 model.

This paper discusses potential solutions to the swell biases identified, including the ongoing wave data assimilation efforts at the NWS.

2. SEASONAL OVERVIEW

In situ wave measurements in this review are acquired from a moored Datawell Waverider buoy in the Hawaiian Islands. The station is maintained and made available by the PacIOOS and Coastal Data Information Program (CDIP) in partnership with the Department of Oceanography at the University of Hawaii. The sampling rate is one hertz (Hz), and the acquisition time is 20 minutes. Significant wave height (H_s), peak wave period (T_p) and peak wave direction (PkDir) are reported on 30-minute cycles. These instruments utilize a stabilized platform sensor to track the vertical component of the orbital wave motion, and are capable of measuring reliable wave height measurements with a resolution up to 1 cm.

The Waimea Bay buoy (51201) data are used in this seasonal overview to evaluate the NWPS wave field output in section three. Station 51201, shown in Fig. 1, is located 7.9 km west of Sunset Point at 21.6705N, 158.1172W. Water depth at the buoy is 200 m.

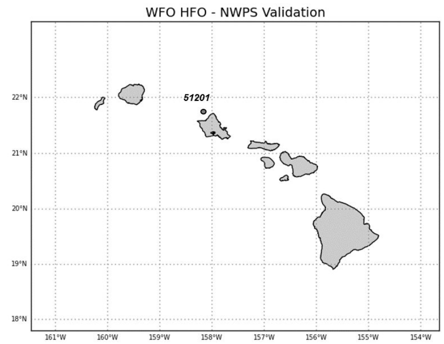

Figure 1. Observations used during the 2016 and 2017 winter months are from the nearshore PacIOOS Waimea Bay buoy (51201), located around 7.9 km west of Sunset Point on the North Shore of Oahu.

Statistics for wave data spanning the entire 2016-2017 winter season at buoy 51201 are presented in Fig. 2a for: H_s, $T_{p,}$ and PkDir. The distributions of these wave parameters from 1376 observations are roughly symmetric and unimodal. The averages are around 2 m for H_s, 12 seconds for T_p and 330 degrees for PkDir, which reflect a near normal winter season for the Hawaiian waters exposed to north Pacific swells. Standard deviations are 0.6 m for H_s, 3 seconds for T_p and 20 degrees for PkDir.

To identify seasonal variability, distributions of H_s observations are also analyzed in monthly intervals through the period with box plots in Fig. 2b. Included in each monthly box plot are: minimum, first quartile, median (yellow line), third quartile, and maximum. November through February are the more active months through the season, with each month displaying a positive skewness relative to the median. Maximum outliers through this peak period range from around 4 to 5 m with a maximum H_s measured in November.

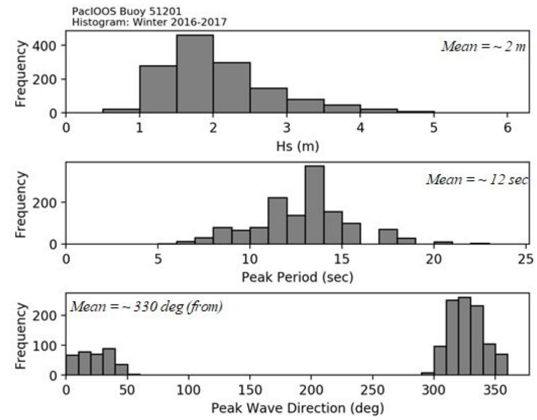

Figure 2a. Histogram displaying data distributions of H_s, $T_{p,}$ and PkDir at buoy 51201 from September 2016 through April 2017.

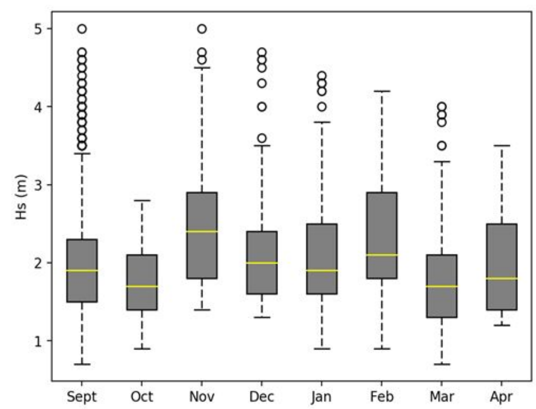

Figure 2b. Box plots displaying monthly data distributions of H_s observations from buoy 51201 from September 2016 through April 2017.

3. MODEL VALIDATION PERIOD – WINTER 2016 - 2017

3.1 *Overview*

The nearshore PacIOOS Waimea Bay buoy 51201 observations are correlated to the modeled H_s and T_p output from NWPS through the 2016 and 2017 winter months covering the September through November period. Model output from November 17, 2016 through December 10, 2016 is discarded due to missing buoy observations (buoy adrift). A total of 1376 data samples are accounted for in the evaluation.

Overall results from the validation period reveal very strong correlations between the observations and model output and generally yield accurate forecast guidance across the nearshore Hawaiian waters. Model biases, however, are shown during significant swell events that typically lead to: phasing offsets between observations and model output and under forecasted swell heights at the peak of the events. These model tendencies will be evaluated in this section using a 12 day period from January 19, 2017 through January 31, 2017 where four consecutive high-impact swell events impact the area.

3.2 *NWPS vs 51201 Observations*

A two-panel time series of modeled H_s (top; red) and T_p (bottom; red) against observations (blue) through the validation period is shown in Fig. 3. The error bars depict the model H_s and T_p differences relative to the observations (red = model over forecasting; blue = model under forecasting). The mean absolute error (MAE) is 0.25 m for H_s and around one second for T_p.

A linear regression analysis including all observations through the period show very strong correlations (r = .885) between the model H_s and observations (Fig. 4). The mean forecast error is -0.02 m for H_s, which implies a slight tendency for the model to under forecast H_s.

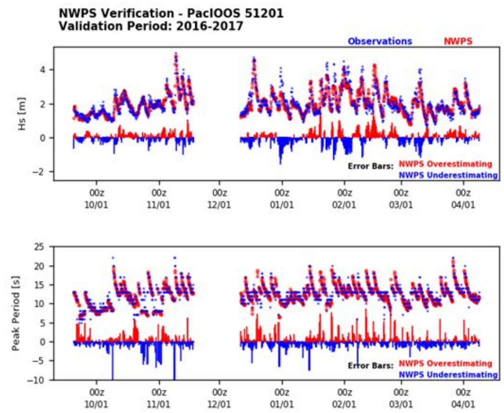

Figure 3. Two-panel time series of the NWPS H_s (top) and T_p (bottom) against real-time observations through the 2016-2017 winter season at buoy 51201. Error bars denote the differences between the model and observations.

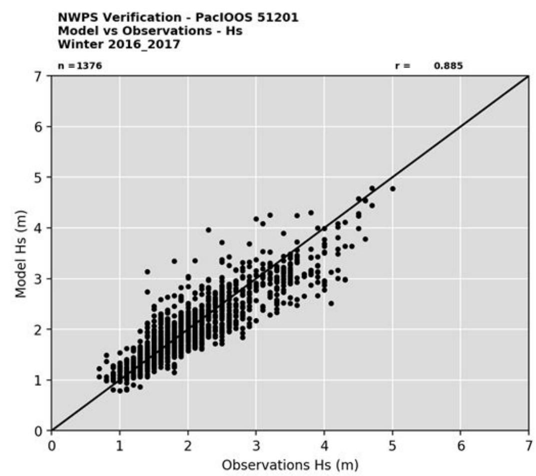

Figure 4. Linear regression analysis showing very strong correlations (r = 0.885) between the modeled H_s and observations.

To determine how the model performs during high-impact events, an error bar chart for H_s is shown in Fig. 5 (top image) that only accounts for H_s observations that are greater than one standard deviation relative to the mean. The blue bars depict when the model under forecasts H_s and red depicts when the model over forecasts H_s. The MAE is 0.438 m for these cases. The mean forecast error is -0.335 m, which highlights the tendency to under forecast H_s, especially during high-impact events where the model rarely over predicts H_s.

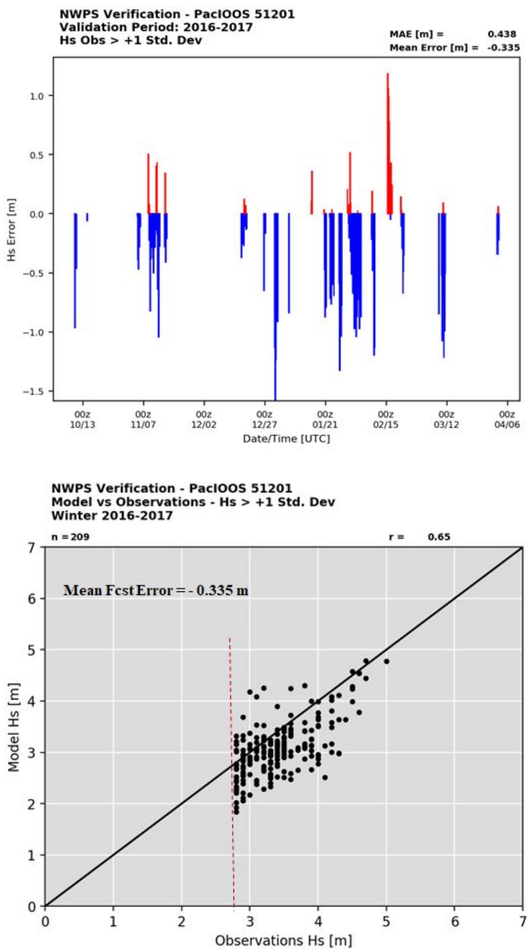

Figure 5. Bar chart (top image) depicting the model H_s error (blue = model under forecasting; red = model over forecasting) at buoy 51201 for significant events defined when the H_s observed is greater than one standard deviation than the mean. The linear regression analysis (bottom image) reveals weaker correlations between the model and observations through the period, which further illustrates the tendency to under forecast (samples to the right of the center line).

3.3 *NWPS vs 51201 Observations: large swell events*

In section 3.2, it was shown that the NWPS output reveals a tendency to under forecast H_s, especially during high-impact events. Since these high-impact events are mostly associated with large swells, with generation sources well beyond the open grid boundaries of the NWPS grid across the northern Pacific, these biases are in turn strongly related to the accuracy of the offshore wave boundary conditions received from the global WW3 model.

Upon further review of individual large swell events, additional systematic model tendencies are revealed through the validation period. These tendencies, on average, include: phasing issues with large swells arriving later than predicted (up to 12-18 hours in extreme cases), modeled H_s converging at a peak below observed (around a meter on average), and the modeled H_s lowering too quickly through the tail of the events. Fig. 6 displays a time series of H_s and T_p over the course of a 12 day period at the end of January to illustrate these tendencies, for four back-to-back large swell events..

In some cases, however, the phasing issues during large swell events are not reflected. In an attempt to distinguish differences between events where phasing is and is not an issue, swell generation regions are compared. Despite some inconsistencies between events, some correlations between phasing issues during large swell events and generation regions are distinguishable. Large west-northwest (290-310 degrees) swells with distant generation regions across the far northwest Pacific, on average, often arrive later than predicted. For the events arriving from the northwest (320-340 degrees) across the far northwest Pacific, no correlations

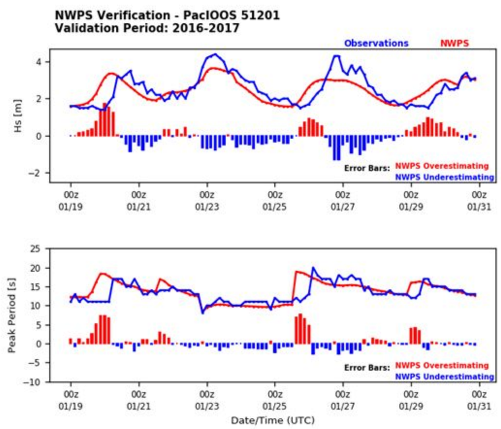

Figure 6. Two-panel time series of the NWPS H_s (top) and T_p (bottom) against real-time observations at buoy 51201 for the January 19-31, 2017 period.

could be made. Some of these northwest swell events reveal strong phasing correlations between the model and observations and some reflect the phasing issues discussed above. In Fig. 7, storm tracks and intensities associated with these more typical northwest swells are shown. Green-colored storm tracks are associated with well forecasted swell events across the Hawaiian waters, whereas, red and magenta tracks corresponded with the events where the swells arrived later than predicted (in the legend, bad (swell arrival 6-9 hours late) and very bad (swell arrival > 9 hours) are defined as modeled H_s and T_p being out of phase with observations).

For swells associated with more nearby sources (< 2000 km) and from distant locations across the north and north-northeast Pacific regions, the phasing issues discussed above from the west-northwest and northwest sources are not revealed. Swell arrival times correlate well with the predictions from the model. However, the low bias of the predicted H_s is shown, especially at the peak of these north and north-northeast events. Fig. 6 presents a northerly swell example associated with a more nearby generation source around January 23, 2017 in the time series (note the higher frequency wave periods (T_p) in the bottom panel through this sequence).

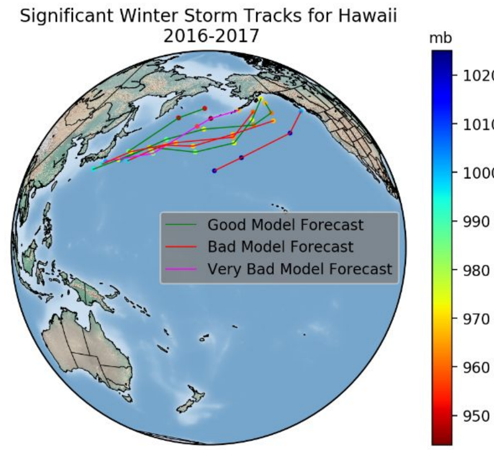

Figure 7. Storm tracks and intensities associated with large swell events over the Hawaiian waters from the more typical northwest direction (320-340 deg). The color-coded points along each track are set at 24 hour increments and specify storm intensity (surface pressure (mb - millibar)). The color of the track denotes whether or not the wave model ended up revealing a phasing issue where the swell arrived later than predicted.

4. DATA ASSIMILATION EFFORTS AT THE NATIONAL WEATHER SERVICE

As a potential future solution to the model biases identified for Hawaii in Section 3, mesoscale wave data assimilation efforts within the National Weather Service (NWS) are introduced in this section. Initial work across the Hawaii region shows positive results, that minimize these model biases in the WW3 output during high-impact events by incorporating buoy and satellite observations.

4.1 *Data Assimilation System Description*

The data assimilation systems provide an analysis of the parameter of interest, by combining observations and the numerical model state; under specific assumptions about their statistical error properties. Several data assimilation algorithms have been suggested over the span of the last 70 years for which there are many implementations. In this case, for the analysis of the significant wave height a 2D-var approach (Flampouris et al. 2016) is used, implemented as Gridpoint Statistical Interpolation, GSI, (Shao et al. 2016) and used for the UnRestricted Mesoscale Analysis, URMA, provided operationally by NCEP/NWS (Carley et al. 2018). In principle the variational data assimilation is an advanced regression analysis, based on the dynamical models and the observations (Bennet, 2005); the novelty lies in the mathematical and physical subtlety of realistic dynamics, in the complexity of the multivariate error fields and the computational challenges, e.g. size of data sets and efficiency.

For this application the model state is provided by the operational wave prediction system of NWS based on the WW3 (Tolman et al. 2002). The background field is produced by merging the significant wave height from the three different operational grid resolutions for wave prediction (Chawla et al. 2013) at the vicinity of HI. The error properties used for the analysis are determined through two years global error analysis of the operational wave prediction.

The main sources of observations are the six NDBC buoys and rarely ships of opportunity; as well as the altimeter observations of significant wave height. Data from the following satellites have been assimilated: Cryosat-2, Jason-2 and Jason-3 and Saral/Altika. The observations from both sources have undergone extensive quality control based on the physical properties of the wave field and the properties of the sensors. For the accuracy of all the observations, the appropriate values from the bibliography and the data providers are used.

The GSI minimizes the distance between the observations and the model state by actually analyzing their difference. This produces the increments, a grid of changes to the first guess, which gets added back to the first guess to give the analysis. The key input to the GSI affecting how closely the analysis will fit the observations and how the error will be spatially distributed is the standard deviation of observations and background error for Hs and the background error covariance. As this is a high resolution analysis, the local geomorphology is taken into consideration through anisotropic covariance (De Pondeca et al. 2011) depending on the local bathymetry.

The spatial resolution of the significant wave height analysis is approximately 2.5 km and it is provided hourly, with a 6 hours delay. The reason of the delayed analysis is the observations latency.

4.2 *Data Assimilation Verification Results in Hawaii*

As a demonstration, Fig. 8 illustrates the applicability of assimilating observations into an analysis field through a four day validation period from December 10, 2017 to December 14, 2017. The top spatial plot in this figure shows the background H_s field (First Guess) from WW3, along with the buoy locations (red dots). The second (middle) plot is the reconstructed analysis field after the observations have been assimilated. The third (bottom) plot is a spatial difference between the

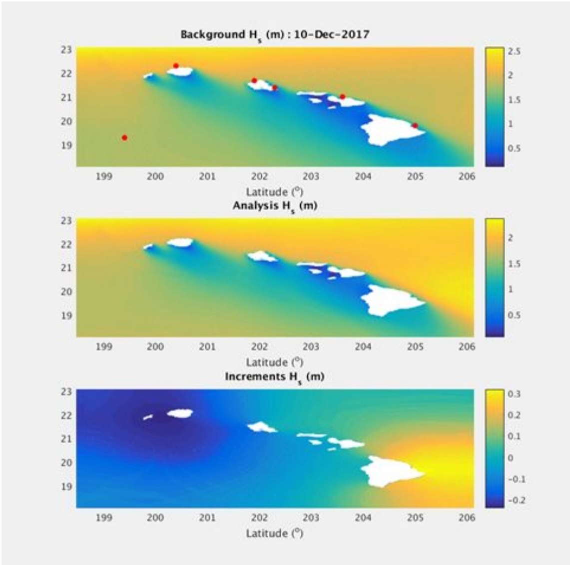

Figure 8. Three-panel spatial plot of the First Guess background WW3 output (top), Analysis (middle), and the spatial differences between the First guess and Analysis (bottom) for parameter H_s.

Analysis and First Guess from WW3. The verification results are highlighted in Fig. 9, which reflects the biases between the model First Guess and the Analysis (top panel), the RMSE (second panel), and the observations include in the analysis field (bottom panel). Considerable improvements are shown in this demonstration and generally yield more accurate representation of the actual wave height conditions, where biases and RMSEs are minimized (red plot in Fig. 9).

5. CONCLUSIONS

Results from the validation period for NWPS in a swell-dominated environment, such as Hawaii, have proven to be applicable and yield generally accurate wave guidance across the nearshore waters. Overall biases, however, reveal a slight tendency to under forecast H_s, especially for high-impact events associated with large swells.

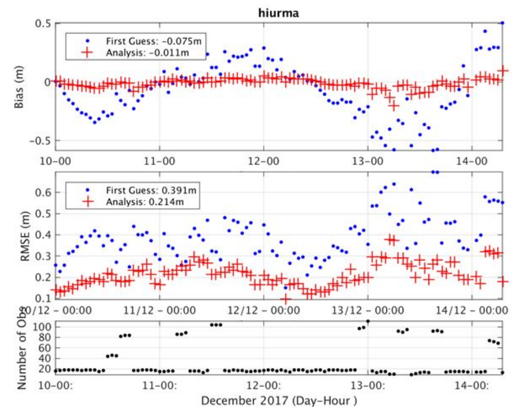

Figure 9. Three-panel time series demonstration reflecting the initial verification results between the First Guess WW3 model output and the Analysis for Hs through the December 10-14, 2017 period, that includes: Bias (top), RMSE (middle), and observations included in the Analysis.

The main challenges discussed for these cases, mainly occur due to input errors at the model open grid boundaries from WW3. For these events, model errors generally follow a systematic tendency that include:

- Swell arrival times predicted too early by the model (six to nine hours on average, with some extreme cases up to 18 hrs)
- Model H_s converges at a peak too low compared to buoy observations (around a meter)
- Model tendency to under forecast H_s as the swells lower through the tail of the events

Although initial attempts to correlate these swell tendencies to storm tracks (generation regions) across the northern Pacific were discussed, additional cases are needed in the future before any conclusive evidence can be drawn from these initial correlations.

As a potential solution to the discussed WW3 boundary condition biases and tendencies reflected from the NWPS verification period, ongoing data assimilation efforts within the NWS were introduced. Initial results across the Hawaii region reveal promising results that minimize WW3 boundary condition biases by reconstructing an analysis field for H_s through assimilating buoy observations and satellite altimetry data. Future work will expand on these efforts through reconstruction of the wave spectra within the global WW3 that initializes NWPS, to test whether this reduces the phasing and low bias issues in NWPS associated with large swell events in Hawaii.

6. ACKNOWLEDGEMENTS

Buoy observations were furnished by the Coastal Data Information Program, Integrative Oceanography Division, operated by the Scripps Institution of Oceanography, under the sponsorship of the U.S. Army Corps of Engineers and the California Department of Parks and Recreation (http://cdip.ucsd.edu).

7. REFERENCES

BENNETT, Andrew. Inverse Modeling of the Ocean and Atmosphere. CAMBRIDGE UNIV PR, 2005.

Booij, N., Ris, R.C., Holthuijsen, L.H., 1999: A third-generation wave model for coastal regions: 1. Model description and validation. *J. Geophys. Res*. 104 (C4), 7649-7666.

Carley J. R., IMSG and NOAA/NCEP/EMC, College Park, MD; and M. Pondeca, S. Levine, R. Yang, Y. Lin, S. Flampouris, J. H. Alves, J. Whiting, S. Melchior, A. M. Gibbs, G. Gayno, R. J. Purser, T. Lei, W. S. Wu, D. F. Parrish, B. T. Blake, C. Guastini, G. Manikin, B. Yang, E. Colón, X. Zhang, E. Rogers, M. Pyle, and J. C. Derber The Continued Development of the NOAA RTMA/URMA Systems at AMS January 2018

Chawla, A., H.L. Tolman, V. Gerald, D. Spindler, T. Spindler, J.G. Alves, D. Cao, J.L. Hanson, and E. Devaliere, 2013: A Multigrid Wave Forecasting Model: A New Paradigm in Operational Wave Forecasting. Wea. Forecasting, 28, 1057–1078, https://doi.org/10.1175/WAF-D-12-00007.1

De Pondeca, M.S., G.S. Manikin, G. DiMego, S.G. Benjamin, D.F. Parrish, R.J. Purser, W. Wu, J.D. Horel, D.T. Myrick, Y. Lin, R.M. Aune, D. Keyser, B. Colman, G. Mann, and J. Vavra, 2011: The Real-Time Mesoscale Analysis at NOAA's National Centers for Environmental Prediction: Current Status and Development. Wea. Forecasting, 26, 593–612, https://doi.org/10.1175/WAF-D-10-05037.1

Flampouris, S., Alves, J.-H, Pondeca, M., Whiting J., 2016. Inclusion of significant wave height analysis to NCEP's UnRestricted Mesoscale Analysis (URMA), Ed. E. Astakhova, Working Group on Numerical Experimentation, WMO

Shao, H., J. Derber, X.-Y. Huang, M. Hu, K. Newman, D. Stark, M. Lueken, C. Zhou, L. Nance, Y.-H. Kuo, B. Brown, 2016: Bridging Research to Operations Transitions: Status and Plans of Community GSI. Bull. Amer. Meteor. Soc., 97, 1427-1440, doi: 10.1175/BAMS-D-13-00245.1.

Tolman, H.L., B. Balasubramaniyan, L.D. Burroughs, D.V. Chalikov, Y.Y. Chao, H.S. Chen and V.M. Gerald, 2002: Development and implementation of wind generated ocean surface wave models at NCEP. *Weather and Forecasting*, 17, 311-333.

Van der Westhuysen, A.J., R. Padilla, P. Santos, A. Gibbs, D. Gaer, G. Dusek, J. Long, H. Stockdon, J. Notchey, and H.L. Tolman, 2016: Implementing the Nearshore Wave Prediction System as a centralized, on-demand marine hazard guidance system. Proc. 96th AMS Annual Meeting, New Orleans, LA.